Journal of Archaeological Science: Reports 18 (2018) 197–212

Contents lists available at ScienceDirect

Journal of Archaeological Science: Reports

journal homepage: www.elsevier.com/locate/jasrep

Geophysics and geochemistry; an interdisciplinary approach to archaeology in wetland contexts

Christine Joan Milton*

School of Archaeology Geography & Environmental Science, University of Reading, Wager Building, Whiteknights, Reading, RG6 6AB, England, United Kingdom

ABSTRACT

Wetlands are a non-renewable resource of high potential for organic archaeological deposits and palaeoenvironmental sequences. This resource is at threat from development and climate change. Only a small percentage of the identified wetlands in North West Europe have been studied with regard to their depth, stratigraphic architecture and the heritage assets they contain. In this paper several case studies are combined to show the variation of radar velocity field with different wetland sediment types. Sediment types are classified based on their physical and chemical properties. The results demonstrate how the application of geophysics can be used to identify archaeological features and interpret them within a wetland landscape. The ground penetrating radar (GPR) response and geochemical signatures given by archaeological structures and palaeolandscape features, presented here improves the quality and reliability of scientific information derived from archaeological prospection in wetland contexts. More accurate values for the dielectric permittivity of different wetland sediments have been calculated, allowing the response of GPR in wetland contexts to be predicted. Geochemical signatures associated with different sediment types and archaeological structures have also been demonstrated. Both GPR and the geochemical analysis of sediment can be employed across the dryland wetland interface bridging the gap between wetland and dryland archaeology and offers a potential to shape global debates regarding how wetland heritage is managed in the future.

1. Introduction

Wetlands are generally rich in cultural heritage due to the unique conditions of preservation (Coles et al., 1973; O'Sullivan, 1998; Van de Noort and O'Sullivan, 2006; Lillie and Ellis, 2007; Menotti, 2012). Decades of archaeological excavations suggest that remains are often fragmentary and deeply buried. This implies that many sites, especially wooden trackways and platforms, and occasionally occupation surfaces and settlements, and industrial debris remain to be discovered. The current management is deemed to be reactionary, attempting to preserve wetland archaeological sites in situ once they have already been disturbed (Chapman et al., 2009). This is costly and in many instances the optimal conditions of preservation cannot be attained or sustained (Amendas et al., 2013; Jones, 2013). Due to a less stable environment wetland deposits are less likely to be preserved in situ successfully than dryland deposits (Van de Noort et al., 2001, and Matthiesen, 2008; Milner et al., 2011). The ongoing pressure on the archaeological resource from environmental change due to development and, arguably, climate change (see Henman and Poulter, 2008), as well as afforestation, means that a shift to proactive management strategies is urgently required to aid the rapid discovery and characterisation of buried wetland archaeology.

This paper presents such an approach using geophysics, geochemical and borehole methods at higher resolution than that previously demonstrated by Utsi (2004), Bates et al. (2007) and Fyfe et al. (2010). By modelling the geochemical and geophysical signature of different targets in a variety of wetland contexts it is possible to address the general scepticism in the academic and commercial archaeological community about the usefulness of geophysics in wetland archaeology. Despite geochemistry having been used as a means of prospecting and characterising anthropogenic sediments in dryland contexts (Persson, 1997 for example), little has been done in wetlands in conjunction with archaeologists to improve understanding of the limitations of individual techniques (Haslam and Tibbett, 2004; Oonk et al., 2009; Eberi et al., 2012).

2. Materials and methods

Five sites associated with an archaeological structure or palaeolandscape were selected for this study (Fig. 1). Each contains one or

* 6 Parsley Close, Earley, Reading, Berkshire, RG6 5GN, England, United Kingdom.
E-mail address: christine.bunting@hotmail.co.uk.

https://doi.org/10.1016/j.jasrep.2017.12.037
Received 12 August 2016; Received in revised form 3 December 2017; Accepted 22 December 2017
Available online 20 February 2018

Fig. 1. Map of North West Europe showing locations of the sites discussed in this paper.

Table 1
Details of each of the case study sites.

Site	Grid reference	Sediments	Local geology	Associated archaeology
Castlegar bog, Galway, Ireland	ING M82610 39213	Ombrotrophic and fen peat	Limestone moraine	Wooden trackway and platform structures
Annaghbeg bog, Galway, Ireland	ING M81986 37210	Ombrotrophic and fen peat	Limestone moraine	Undisturbed palaeoenvironmental sequences
Shapwick Heath, Somerset, England	NGR ST42204020	Fen peat	clays and sandy outcrops of interglacial Burtle Beds	The Sweet Track (Coles et al., 1973; Wells et al., 1999)
Caldicot, Monmouthshire, Wales	NGR ST4870088674	Alluvial clays and peat beds	Old Red Sandstones and Carboniferous beds	Wooden structures dated to the Bronze Age (Nayling and Caseldine, 1997)
Marsal, Lorraine, France	E 6°36′29″ N48°47′22″	Alluvial clays and peat beds	Lower Keuper Marl (a salt-bearing formation)	Iron Age salt workings (Olivier and Kovacik, 2006; Riddiford et al., 2012)

more sediment types that are typically found at wetland archaeological sites (Table 1). At Shapwick, Castlegar and Caldicot the case study objective was to detect evidence of trackways continuing from areas previously excavated and to improve the understanding of the local stratigraphy. Two additional case studies where the objective focused on local stratigraphy alone were made at Annaghbeg bog and Marsal, the velocity profiles are included here but for more details the reader is referred to Milton (2015).

Slightly different combinations of methods were employed at each site, from long transects covering a large area (for which data may already have been acquired, see Hodgson et al., 2009) to grids with data collected at a spacing of 0.125 m for the 400 MHz antennae and 0.25 m for the 200 MHz antennae. This is greater than the sampling frequency suggested by Historic England (formerly English Heritage) but does not meet the Nyquist limit; by sampling the grids more densely more convincing data might have been obtained. This demonstrates that while for this research the collection parameters were kept as similar as possible across all sites, in order to allow direct comparisons to be made, the approach can be much more flexible allowing it to be tailored to the sensitivity and size of the site.

At each site a grid of ground penetrating radar (GPR) data was collected using the Radan SIR20 software and GSSI hardware, utilizing 200 MHz and 400 MHz common offset antenna set up using the parameters in Table 2. At Annaghbeg and Shapwick long profiles were

Table 2
Data collection parameters used for both the 200 MHz and 400 MHz antenna.

Parameter	200 MHz	400 MHz
Samples per scan	512	512
Dielectric constant	10	10
Time zero correction	auto	auto
Time window	150	100
Scans per metre (using odometer)	50	50
Transect (trace) spacing	0.5 m	0.25 m

collected across the sites using the 200 MHz antenna prior to this to identify the most suitable position for the grid. This step was not necessary at the other sites as prior survey or excavation was used to select an appropriate location for the grid. Data for each grid was collected in two directions perpendicular to each other to ensure maximum coverage. An automatic gain control (AGC) was applied during collection of the data. It has been argued that AGC has limited use in archaeology and that using a fixed gain curve is better (Leckebusch, 2003). However, it was observed in the field that an appropriate AGC gain, with manual adjustment to avoid any over gain, set up for each site achieved greater depth of penetration and returned signal to noise ratio. An example of the gain values used is 2, 32, 49, 59, 61, 63, 66 and 67 dB at regular intervals of 18.75 ns over a range of 150 ns. To ensure no clipping of the data collected the gain for each grid was set at a location where the highest amplitude was observed when moving the antennas over the area to be surveyed (Conyers, 2004, pp93).

Velocity determination is an essential part of this research, during data collection an arbitrary value of 10 for the dielectric permittivity was used (Table 2) which was corrected in post-acquisition processing. At most sites the two-way travel time to a point reflector was used to calculate this by inserting a metal corer into the ground to a known depth. An additional common mid-point (CMP) survey at Shapwick was carried out due to the wider variety of sediment types encountered. This was completed using Pulse EKKO 1000 GPR console with 225 MHz and 450 MHz antennas provided by the NERC Geophysical Equipment Facility (GEF); Loan 991. These antennas are housed separately allowing the offset between the transmitting and receiving antennae to be increased. This was followed by the collection of a set of two cores at the centre points of each gather. The 225 MHz antennas were set over each of the three target points with a minimal separation of 0.5 m and data were acquired at antenna separations increasing in 0.1 m steps, to a maximum separation of 8 m. This process was repeated for the 450 MHz antenna with an initial separation of 0.25 m, step size of 0.05 m and maximum separation of 4 m.

Data collected using the SIR20 system has some processing steps applied on collection including a simplified high pass filter to dewow the signal. Further processing in Radan 7 included adjusting the time zero to the first positive peak and a triangle FIR filter to remove any background noise. All the vertical traces collected from each grid were combined to give a 3D block of data from which horizontal 'time-slice' images of the area were taken following a Hilbert transform for magnitude. Horizontal stacking has been applied to longer traces in order to remove noise and allow complete transects to be displayed. Topographic correction was also applied to longer traces where there is a large change in slope over the area being surveyed. The CMP data collected was imported to Reflexw (Reflexw, 2012) software and basic 2D processing including dewow, time zero correction and a gain were applied. They were then analysed in the CMP module using the semblance analysis to help identify weaker signals.

As geophysical surveys are only a relative means of detection, each of the survey areas has had samples collected for ground validation. Cores were collected from locations of interesting anomalies within the grid and were described using Tröels-Smith (1955) and the Munsell colour chart. Bulk samples were taken using an 8 cm sample interval and analysed for moisture content, loss on ignition determination, humification and particle size analysis. Moisture content, organic matter content and bulk density samples were determined using the gravimetric technique (Bengtsson and Enell, 1986). Humification was measured following the technique outlined for palaeostudies (Chambers et al., 2011). Particle size was analysed using a Beckman Coulter LS230 laser granulometer following random sub-sampling and disaggregation in calgon. Pore water was extracted from the sediment in the laboratory following a procedure modified from Dewis and Freitas (1970) and Sharpley et al. (2008), this was found to be the most effective technique after some modification (see Milton, 2015). Each of the samples was analysed for electrical conductivity (using a Hanna HI8820N conductivity probe), pH (using a Hanna H18424 probe calibrated in pH buffers 7 and 4) and multi-element analysis using ICP-OES. These results have allowed a more complete interpretation of the GPR data.

3. Theoretical background

It is important to establish the dielectric permittivity of the sediment in order to convert the time it takes for the EM wave to travel to the target and back into a depth estimate. While it is strongly recommended that this is calculated for each site, in practice quoted figures such as those below are often used to give an approximate calculation when anticipating if the results will justify the survey. Davis and Annan (1989), Mussett and Khan (2000), GSSI (2002), Conyers (2004), and Styles (2012) all give tables of dielectric permittivity for a range of sediments and materials (Table 3). It can be seen that these values, particularly those for wetland sediments, have large ranges and peat is noticeably absent making it difficult to model results.

Imprecise estimates of dielectric permittivity also make it difficult to predict both longitudinal and lateral resolution, and the reflectivity of targets. The minimum size of a target can be calculated using the values for wavelength and velocity where the wavelength (λ) is calculated as the speed of light (c) divided by the central frequency of the antenna (f) multiplied by the square root of the dielectric permittivity of the sediment (K);

$$\lambda = \frac{c}{f\sqrt{K}}$$

Vertical resolution is assumed to be greater than or equal to quarter of the wavelength (English Heritage, 2008) whereas the lateral resolution (Δl)also depends on the depth (D) due to the spreading of the EM wave as it travels away from the antenna;

Table 3
Dielectric permittivity (and velocity of the EM wave in m/ns) for a range of sediments taken from Conyers (2004), Mussett and Khan (2000) and Styles (2012), For Mussett and Khan (2000) and Styles (2012).

Material	Conyers (2004)	Mussett and Khan (2000)	Styles (2012)
Air	1	1 (0.30 m/ns)	1 (0.30 m/ns)
Fresh water	80	81 (0.033 m/ns)	80 (0.033 m/ns)
Sea water	81–88	81 (0.01 m/ns)	81 (0.01 m/ns)
Ice	3–4	2–3 (0.16 m/ns)	3–4 (0.16 m/ns)
Clay	5–40	(wet) 25–40 (0.5–0.6 m/ns)	5–40 (0.06 m/ns)
Silt	3–30	5–30 (0.07 m/ns)	5–30 (0.07 m/ns)
Silt (saturated)	10–40		
Sand (dry)	3–5	3–6 (0.15 m/ns)	3–5 (0.15 m/ns)
Sand (wet)	20–30	20–30 (0.06 m/ns)	20–30 (0.06 m/ns)
Marsh/forest land	12		
Dry sandy coastal land	10		
Organic rich surface soil	12		
Organic rich agricultural land	15		

Table 4
Wavelengths (taken from Conyers, 2004; 60) and vertical detection limit for the 200 MHz and 400 MHz antenna in different medium, and lateral resolution at the depth of 1 m.

Medium	Dielectric Permittivity, K	200 MHz λ	400 MHz λ	Vertical 200 MHz	Vertical 400 MHz	Lateral 200 MHz	Lateral 400 MHz
Fresh/sea water	81	0.168 m	0.084 m	0.042 m	0.021 m	0.153 m	0.132 m
Wet clay/silt	40	0.237 m	0.119 m	0.059 m	0.029 m	0.219 m	0.189 m
Wet sand	30	0.274 m	0.137 m	0.069 m	0.034 m	0.255 m	0.220 m
Marsh/forest	12	0.433 m	0.216 m	0.108 m	0.054 m	0.410 m	0.356 m

$$\Delta \boldsymbol{l} \geq \frac{\boldsymbol{\lambda}}{\mathbf{4}} + \frac{\boldsymbol{D}}{\sqrt{(\boldsymbol{K}-\mathbf{1})}}$$

It is important this aspect can be modelled as accurately as possible as it impacts on the requirements for resolution when collecting the data. Given the dielectric permitivities given in Table 3 and considering the dimensions of a typical trackway (1-2 m wide and of variable length) or paleo-landscape target (usually at least several metres in length) both a 400 MHz and 200 MHz antenna should be able to detect such features in all wetland sediment as the greatest vertical and lateral detection limits are 0.108 m and 0.410 m respectively (Table 4).

The coefficient of reflectivity (R) can be calculated where K_1 is the dielectric permittivity of the overlying sediment and K_2 is the dielectric material of the underlying sediment (Davis and Annan, 1989);

$$R = (\sqrt{K_1} - \sqrt{K_2})/(\sqrt{K_1} + \sqrt{K_2})$$

From this it can be predicted that water over marsh will give a stronger reflection than water over clay or silt or sand with moderate negative reflectance values (i.e. the polarity of the reflected wave has been reversed) for marsh over sand, clay and silt (Table 5).

GPR reflections are caused by changes in dielectric permittivity, which is often determined by conductivity (largely related to water content) and the magnetic properties of the sediment. A water content difference of > 5% is expected to give a response (Theimer et al., 1994). Three key components of sediment that produce a reflection are moisture content, complex conductivity and humification, where changes in humification produce a change in the dielectric permittivity, probably due to a change in porosity and therefore water content (Kettridge et al., 2008). It is therefore reasonable to expect detection of archaeological structures constructed using wood (or other materials) and changes in sediment type and humification by GPR. Models such as Topp et al. (1980) and CRIM formula are used to calculate moisture content from dielectric permittivity. Water content calculated from the dielectric permittivity using models, which are not calibrated to field scale, are unreliable for organic rich and clay rich sediments (Friedman, 1998). The results presented in this paper allow a comparison of gravimetric water content values and those calculated from dielectric permittivities measured in field using the Topp and CRIM models demonstrating the degree of this inaccuracy.

Although the size and characteristics of anomalies can suggest the presence of an archaeological structure or landscape feature, GPR is a remote technique which needs ground truthing. Physical and geochemical characterisation of deposit types through analysis of material collected from boreholes was essential to interpreting the GPR data. Geochemical indicators related to human occupation are used to characterise sites in dry land situations, with phosphorus (or variants of; Holliday and Gartner, 2007) the most widely used geochemical indicator of human occupation by geoarchaeologists as it is one of the most common chemical outputs of human activity (Conway, 1983; Crowther, 1997; Parnell et al., 2001; Farswan and Nautiyal, 1997; Leonardi et al., 1999; Terry et al., 2004). This approach does not seem to have been widely adopted in wetland archaeology, although one noticeable exception is the analysis on trackway material within the peat bogs of central Ireland which found high phosphate concentrations associated with trackway material (Young et al., 2011a, 2011b, 2011c; Young et al., 2012a, 2012b, 2012c). However, these results were inconclusive due to a limited number of samples which did not allow background variations to be modelled. The sampling strategy adopted here allows the background variations with depth to be taken into account.

Table 5
The reflectivity of wetland sediments, using the dielectric permittivity values given in Table 1.

Overlying material	Underlying material	R value
Fresh/sea water (81)	Marsh (12)	0.44
Fresh/sea water (81)	Wet sand (30)	0.24
Fresh/sea water (81)	Wet clay or silt (40)	0.17
Marsh (12)	Wet sand (30)	− 0.23
Marsh (12)	Wet clay or silt (40)	− 0.29

In wetlands archaeological contexts are often more deeply buried and are liable to have a more complex geochemical nature due to the presence of a fluctuating water table interacting with the context and any underlying or overlying depositional material. It is therefore important to be aware of and to be able to model the geochemistry of the full sediment sequence, for example:

a. Ombotrophic bog: Magnesium concentration higher than calcium (Clymo, 1983)
b. Fen bog: Calcium concentration higher than magnesium, higher iron concentration and lower aluminium concentration than ombrotrophic bog due to the presence of ground water.
c. Alluvial clay: high concentrations of aluminium and iron
d. Marine clay: high concentrations of sodium, sulphate and iron and higher conductivity
e. Sands/gravels: high calcium concentration

A peak in iron concentration is also expected at the maximum height of the water table, below which concentration decreases with depth due to the sensitivity to redox state and pH in bogs (Mighall et al., 2004).

Phosphate analysis alone cannot be relied upon to show evidence of past human activity in wetland deposits as it is highly soluble and prone to leaching (Patrick and Mahapata, 1968). Even in dryland deposits it does not always detect the presence of anthropogenic activity, as in the case of inhumations in the famous ship burial at Sutton Hoo, phosphate analysis twice failed to detect the presence of a body (Bethell and Smith, 1989). Therefore a suite of elements was analysed for this research, based on the findings of research carried out in dryland contexts summarised below.

Calcium, phosphorus and potassium are generic indicators of anthropogenic activity in dryland contexts. Elevated concentrations of calcium and phosphorus indicate substantial and sustained human occupation including the use of fertilisers on arable land and the presence of hearths (Konrad et al., 1983; Entwistle et al., 1998; Entwistle, 2000; Sullivan and Kealhofer, 2004; Wilson et al., 2008). Potassium (also thorium, rubidium and caesium although little is understood of these latter three) is also used as an indicator of human occupation in 18th century Scottish habitation sites (Entwistle et al., 1998; Entwistle, 2000). Copper, manganese, iron and lead are indicative of specialist activity areas such as craft and tool sharpening (Terry et al., 2004). It is perhaps unlikely that tool working would have been an activity

associated with wetland structures. However, if these structures were used as access to wetlands for hunting purposes, it would not be unreasonable to assume that sharpening of tools and loss of tools would have taken place, ritual deposits of metal objects in wetlands are also well documented (Bradley, 1990). Copper is thought to be immobile in ombrotrophic peat and is associated with refuse and excreta (Entwistle et al., 1998; Entwistle, 2000). High concentrations of magnesium are found in association with hearths (Konrad et al., 1983; Entwistle et al., 1998 and Entwistle, 2000). The use of fires or hearths on platforms as opposed to the trackways themselves is more likely, possibly in association with drying peat for fuel. Therefore a peak in any of these elements, or divergence from background variations (ratios), associated with brushwood or more substantial pieces of wood, is likely to indicate a human influence.

4. Results

In all cases the use of GPR coupled with analysis of sediment collected from boreholes improved the interpretation of the sedimentary sequence and the associated archaeology within its context. The 200 MHz data proved to be much more useful for detecting features at depth than the 400 MHz data and, unless otherwise indicated, is the data presented here. Sediment logs have been simplified for presentation here, more detailed (using the Tröels-Smith convention) descriptions can be found in Milton (2015).

At Shapwick an anomaly consistent with the location of the projected course of the trackway (Fig. 2A) is present in a west to east GPR profile north of the interglacial Burtle Bed (Fig. 2D). South of the Burtle several point anomalies were located close to the projected course of the trackway. Within the grid, set up in to investigate this area further, a discontinuous high amplitude linear anomaly orientated approximately north-south was identified on the same alignment as the trackway at a depth of 76.8–99.2 ns/1.92–2.56 m (Fig. 2E and F, 3C and 3D). It has a similar signal to the trackway identified in GPR data by Armstrong (2010) in the bunded area to the north of the area of current investigation where the location of the trackway is well documented (Fig. 2C). The fragmentary nature of this anomaly is likely due to several factors, two of which could be overcome by altering the methodology. The depth of the trackway at this location is at the point where there is a clear demarcation of the signal to noise ratio, which can clearly be seen at around 70 ns in Fig. 2D, the use of a lower frequency antenna may give an improved signal to noise ratio at this depth, however the large peak in conductivity at around 1.3 m (Fig. 4E) will limit the quality of the data for any antenna frequency and lower frequency antennas will give lower resolution data. Even at the shallower location surveyed by Armstrong (2010) the anomaly is fragmentary in nature (Fig. 2C). Denser cross-line spacing would likely improve these results at the cost of increasing the time needed to complete the survey. It must also be remembered that trackway structures are often fragmentary in nature, particularly if poorly preserved, and can be difficult to identify even in excavation. Often many sections need to be excavated and compared in post-excavation to identify alignments of longer structures.

The interglacial Burtle Bed itself is clear in a north to south profile collected along a monitoring transect set up by Jones (2013) (Fig. 3B). This is the deepest anomaly detected by the 200 MHz antenna at 130 ns (4.36 m). This was for a strong contrast in sediment type and dielectric permittivity, with dry fen peat overlying sandy clay (Fig. 3A), during favourable dry conditions. Another anomaly identified at Shapwick was a 'U' shaped feature to the north of the Burtle near the location of the unexcavated portion of the trackway (Fig. 2B). This was initially interpreted as a palaeochannel associated with the structure and possibly the reed peat layer identified by Jones (2013). However, analysis of the borehole material and the additional CMP data collected at this point during wetter conditions showed no evidence for this feature. It is therefore apparent that this was the depth the water table had dropped to during the dry season. This depth is below that of the projected trackway, demonstrating this structure is at serious risk of degradation, and the ability of the GPR combined with an initial set of detailed sediment logs to identify such a risk. It also demonstrates how a small error in the dielectric permittivity can lead to large errors in depth estimates. The depths in metres of these anomalies are based on an average EM velocity of 0.067 m/ns, calculated from a returned signal from a redox probe buried at a depth of 1.5 m (Fig. 3E). Depths are therefore likely to be overestimated due to changes (increases) in water content down the sequence.

Due to the range of sediments, and therefore dielectric permittivities, at this site an additional CMP survey was carried out alongside the collection of boreholes at three locations based on the original survey points (SHAPA, SHAPB and SHAPC, see Fig. 2A). This suggested a two layer velocity model, however, the velocity field is liable to be more complex than this and more work needs to be done to create a more comprehensive model (Table 6 and Fig. 4).The sediment was categorised into six broad types; with geochemical analysis used to aid interpretation of SHAPC (Fig. 4E). The Burtle Bed is classed as sandy clay with an EM velocity of 0.07326 m/ns at SHAPB this is overlain by colluvium with a velocity of 0.05656 m/ns. The peat to the north of the Burtle is mainly well humified fen peat with an associated velocity of 0.04458–0.04225 m/ns. Where the surface is dry (up to 0.51 m/10.10 ns) the velocity increases to 0.04813–0.05060 m/ns, closer to that seen in the previous survey. South of the Burtle the peat was considerably wetter at the surface with a slower velocity of 0.04173–0.04244 m/ns. There is also a layer of wood peat containing some large pieces of wood at 1.27 m–0.36 m which is characterised by a spike in conductivity, calcium, magnesium, manganese, sodium and sulphate concentrations. This sediment has an associated velocity of 0.03960 m/ns. The high conductivity of this unit limits any further penetration by the GPR. However, the geochemistry reveals raised calcium carbonate content, conductivity and concentration of sodium at 1.96–2.78 m associated with large pieces of wood. The transition of peat to the underlying clay is at 3.45 m at this location.

At Castlegar anomalies interpreted as trackway material in the 200 MHz data time slices at 38.4–62.4 ns (0.64–1.04 m) suggest the trackway has an east to west orientation linking the East sighting to the northernmost West trackway sighting (Fig. 5D). Another linear anomaly at 48–67.2 ns (0.8–1.12 m) suggests a northeast to southwest orientation linking the East trackway sighting with the southernmost West trackway sighting (Fig. 5E). The most plausible explanation is that there are two features one overlying the other as suggested in the section created by an adjacent drainage ditch (Fig. 5B and C). In the core at 0.96–1.04 m there is a sharp dip in moisture content with an associated increase in bulk density and calcium carbonate content, this is at a similar depth as round woods identified at 0.92–1.00 m. There is also a significant change in sediment properties to near surface conditions at 0.72–0.80 m (Fig. 6C). This adds strength to the argument for two separate structures, one overlaying the other. Both appear to sit on or in stratigraphic horizons in the peat sequence (Fig. 6B). This could demonstrate that the structures were built as a response to changes in stability of the bog surface or may be due to post depositional processes causing the structures to sink down to these horizons. The fragmentary nature of these structures can be seen in Fig. 5B and C, by increasing the density of the cross line spacing when collecting the GPR data the gridding artefacts seen in Figs. 5D and E would be removed making the relationship between the two structures clearer.

This sequence includes an additional sediment type, to those encountered at Shapwick Heath, of ombrotrophic (moss) peat. A core inserted at a depth of 1 m reveals this highly waterlogged moss peat has an EM velocity of 0.033 m/ns (Fig. 6A) and a similar velocity field was found for the adjacent, unmilled, Annaghbeg bog (Milton, 2015). In addition to the trackways four potential stratigraphic boundaries are seen in the GPR data (Fig. 6B). Chemical analysis down the core gives a more complete understanding of the sequence. The geochemistry shows

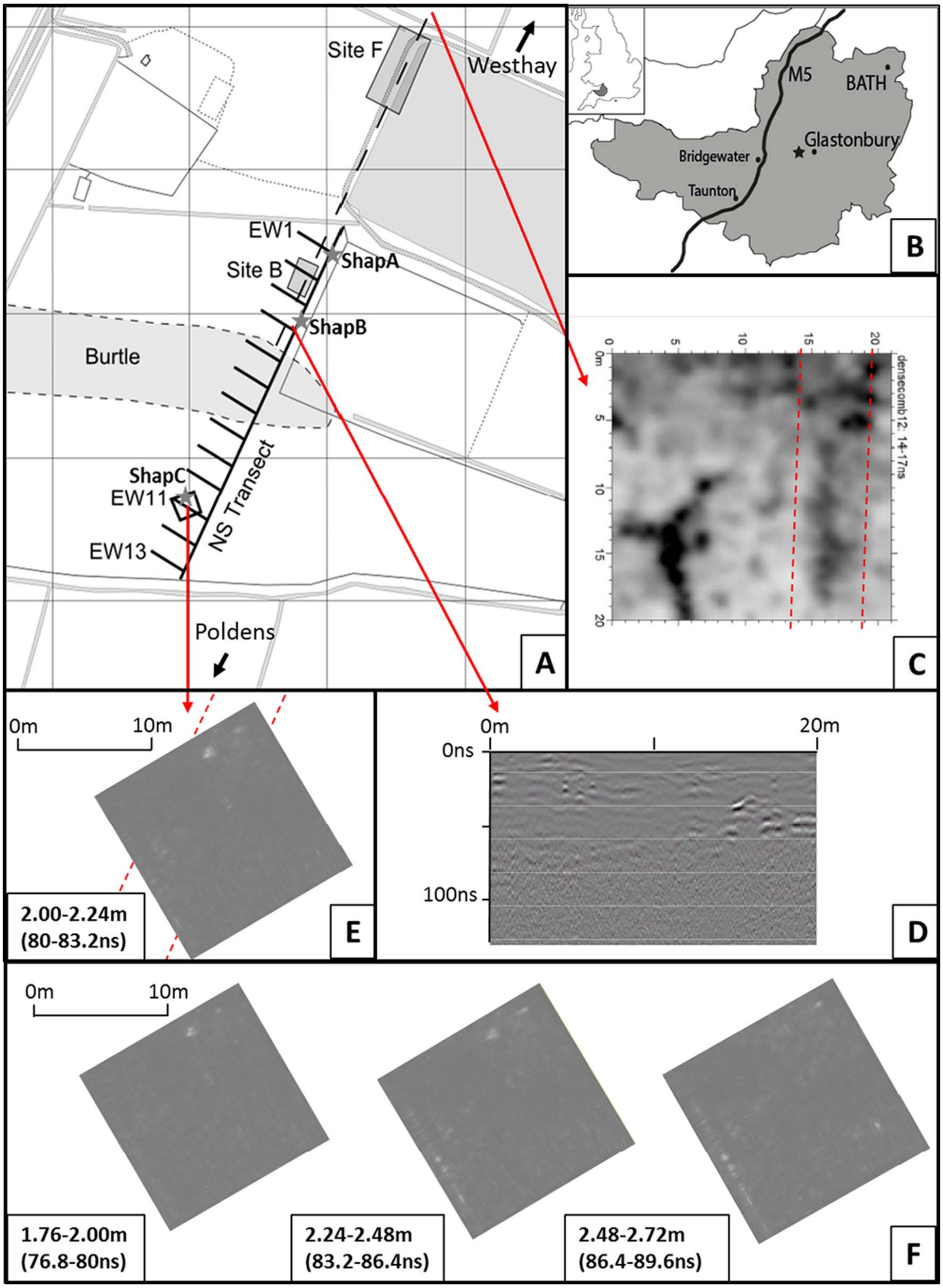

Fig. 2. A; The survey area at Shapwick Heath, showing locations of GPR profiles and grid (solid black lines), locations of cores Shap A, B and C (black stars) and projected course of the trackway (dashed line). B; Shapwick Heath in Somerset. C; Timeslice from Armstrong (2010), the black area (of low amplitude) is a tree root and the area between the red dashed line is the trackway. D; West-east profile with anomaly interpreted as a cross section of the trackway. E and F; Time slice from the grid of data south of the interglacial Burtle Bed, red dashed lines indicate the projected course of the trackway. Black indicates high amplitude and white indicates low amplitude in D and E. (For interpretation of the references to colour in this figure legend, the reader is referred to the web version of this article.)

general trends outlined above with high iron and calcium (with high pH) at the base of the sequence introduced from the underlying geology in groundwater, the Ca:Mg ratio is 1:1 at 2.08 m indicating the depth of the fen (herb) to bog (moss) transition. This is the deepest of the stratigraphic horizons indicated by the GPR at 130 ns (2.17 m) (Fig. 6B and C). High concentrations of aluminium, copper and zinc at 0.08–0.32 m are indicative of redox processes at the water table. The two points in the core where concentrations vary from the general

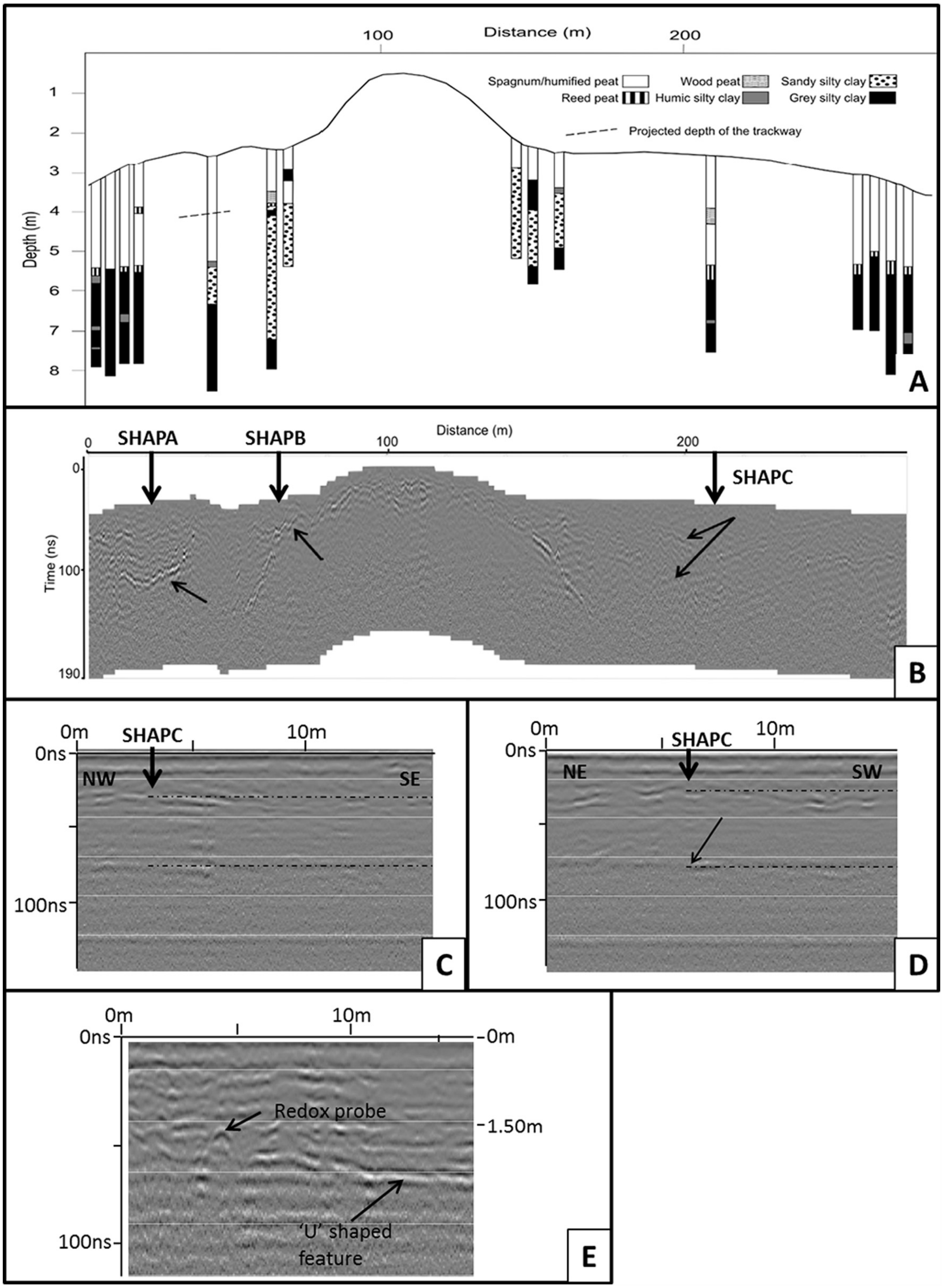

Fig. 3. A; Survey transect set up by Jones (2013) with stratigraphic units, the location of this transect is the same as the long north-south GPR profile shown in B; The north-south GPR profile across the survey area, the interglacial Burtle Bed can clearly be seen in the GPR data as can a 'U' shaped feature adjacent to 'Shap A'. C and D; profiles from the grid of data (see Fig. 2A for location), dashed lines indicate depth of stratigraphic features, small arrow indicates location of potential trackway target. E; profile used for calculation of dielectric permittivity during initial survey, the archaeological sensitivity of this site meant a redox probe already in the ground had to be used as coring in this area was prohibited.

trends are 0.96–1.12 m, where there is a rise in phosphorus concentration to 424.36 μg/L (values similar to those seen on the surface and breaking the correlation with concentration of potassium), and 0.56–0.72 m where there is a peak in concentration of a range of elements (Al, Ca, Cu, Fe, K, Mg and Na) (Fig. 6C). These two depths are at the depths of anomalies interpreted as trackways in the GPR data (Fig. 6B and 5D and E). Between 1.25 m and 1.75 m there is a higher than average concentration of sulphate (Fig. 6C), the top and base of this unit are shown in the GPR data (at 75 ns and 105 ns; Fig. 6B) but no significant change in sediment properties was observed when

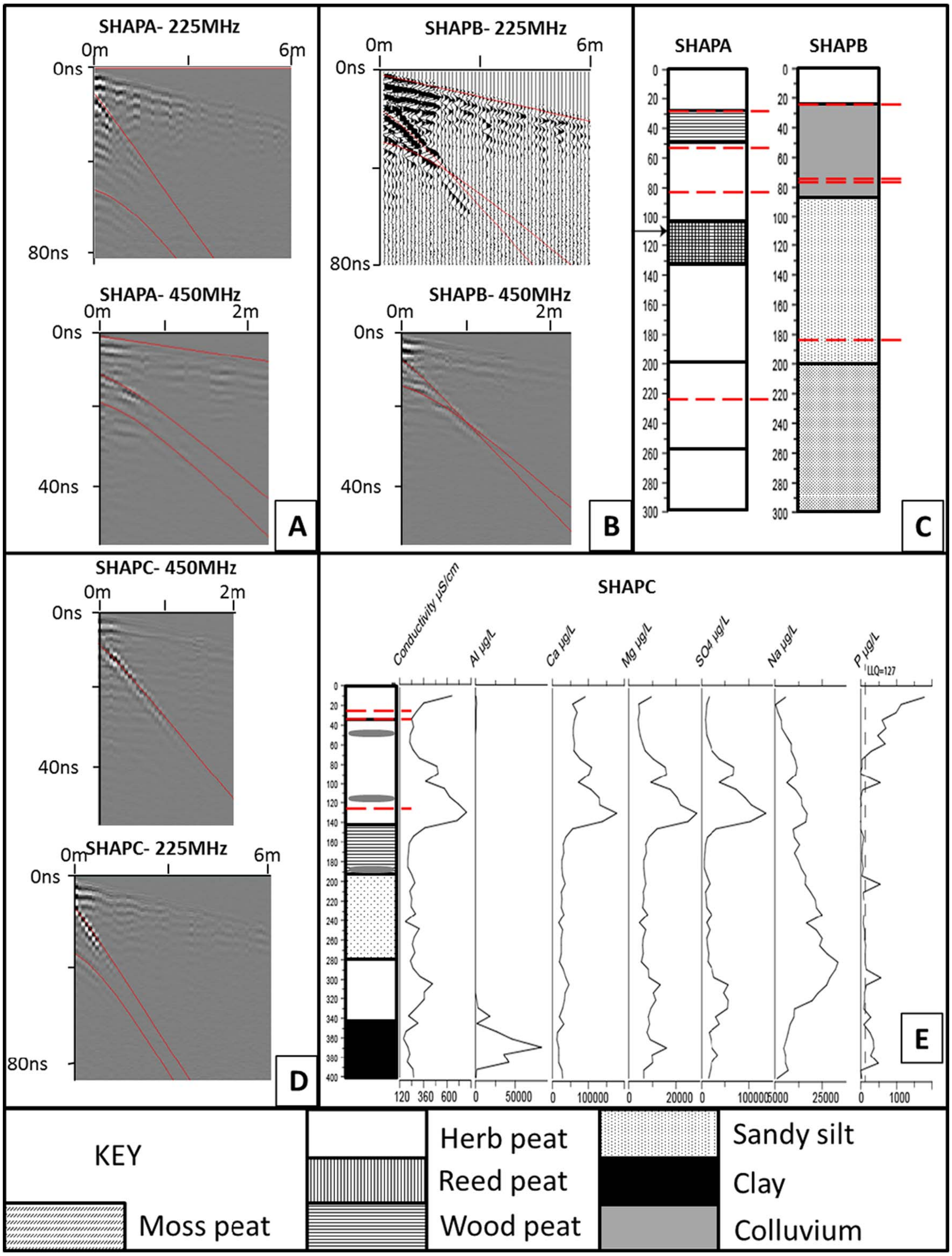

Fig. 4. A; CMP profiles at SHAPA. B; CMP profiles at SHAP B. C; Borehole logs from SHAPA and SHAPB. D; CMP profiles at SHAPC. E; The geochemical profile and borehole log at SHAPC.

describing the core.

At Caldicot (Fig. 7A) and Marsal (see Milton, 2015), the alluvial clay rich sites, the GPR results were severely depth limited due to attenuation of the EM wave (Fig. 8). The velocity of the EM wave in these clay contexts was calculated as 0.05 m/ns, giving a dielectric permittivity of 35.95 (within the range given by Mussett and Khan, 2000 for wet clay) for both sites. However, there is less confidence in this value due to attenuation making the reflection from the corer (at 1 m depth) less clear (Fig. 8B). Despite this, at both sites near surface features were identified (to a depth of no > 1 m); at Caldicot this included a modern trackway consisting of gravel and sand, wood roots and a possible Iron Age structure (Fig. 7B and 8A). At Marsal these were post medieval earthworks, the occupation horizons in association with a palaeochannel which were the target of prospection were observed in the boreholes at a greater depth than the GPR could penetrate (Riddiford et al., 2012). However geochemical analysis allowed the depth of deposits associated with a saltwater spring to be identified (Milton, 2015).

At Caldicot anomalies in approximate alignment to the structure

Table 6
Summary table of the velocities and depths of material and stratigraphic horizons depicted by the CMP analysis.

	X, velocity (m/ns)	Y, depth (ns)	Depth (m)
ShapA 225 MHz			
1 (ground wave)	0.04813	5.78337	0.28
2	0.04458	49.684	2.24
ShapA 450 MHz			
1(ground)	0.05060	10.105	0.51
2	0.04225	17.551	0.82
ShapB 225 MHz			
1 (ground/peat)	0.05656	13.933	0.79
2 (sand/clay)	0.07326	27.865	1.81
ShapB 450 MHz			
1 (ground/peat)	0.04742	5.50832	0.26
2	0.05595	14.393	0.76
ShapC 225 MHz			
1 (ground/peat)	0.04244	8.43813	0.36
2 (wood)	0.03960	31.643	1.27
ShapC 450 MHz			
1 (ground)	0.04173	6.01379	0.25

excavated in Area D were observed at 0.16–0.56 m (Fig. 7B, 8A and C). This is interpreted as an extension of the Iron Age post alignment found during the excavations and for which Mansfield (2009) identified a northern extension (Fig. 7B). The cause of this anomaly appears to be a layer of organic material holding higher water content than the surrounding clay (Fig. 8D). This fits with the faintness of the GPR signal in the data block. Mansfield (2009) suggested a stone strew could also be the cause of the anomaly in her data but this is likely to have resulted a much more distinct signal with small hyperbola caused by individual elements similar to that seen for the modern path in this data set (Fig. 8C). There is also a peak in phosphorus to 449.77 μg/L at 0.32–0.48 m, this along with the presence of charcoal flecks and a crumb structure supports the interpretation of this feature as a palaeosol. The peak in concentrations of aluminium, iron, zinc, copper, potassium, magnesium and manganese at 0.16–0.32 m may be associated with the Iron Age structure but could also indicate the depth of the water table (Fig. 8D).

5. Discussion

A summary table of the velocities calculated during this research is given below (Table 7). The results of this research demonstrate a range of velocities of the electromagnetic wave through different wetland sediments. In peat the water content, and therefore dielectric permittivity, can be highly variable if not waterlogged. The values for different types of sediment are therefore best presented as waterlogged values where possible with additional values given for different degrees of wetness, including dry, where these have been measured.

High humification is associated with lower dielectric permittivity, the ombrotrophic peat at Castlegar and Annaghbeg both had higher dielectric permittivity values than the fen peat at Shapwick Heath (even when highly saturated). The values for the peatlands compare well to that found by Kettridge et al. (2008) of 0.0346 m/ns (below the water table), Kowalczyke et al. (2014) of 0.042–0.039 m/ns for fen peat, and Plado et al. (2011) of 0.036 m/ns with dielectric permittivity of 69.7 (range of 0.034–0.039 m/ns and 60.1–75.7) in ombrotrophic peat. Plado et al. (2011) observed almost no difference in measurements between summer and winter; however, the results of this research demonstrate that the degree of waterlogging does have an impact on the dielectric permittivity in fen peat (Table 6). From the initial survey at Shapwick Heath a velocity of 0.067 m/ns was calculated, this was during exceptionally dry ground conditions (Bunting, 2012). This is substantially faster than that found using CMP in much wetter conditions where slower velocities of 0.04–0.05 m/ns with different values for different classes of peat were found.

Clay and silt minerogenic sediments have lower dielectric permittivity than any of the peat deposits. It is clear that although both peat and clay deposits are fully saturated the peat has the capacity to hold more water than minerogenic sediments due to the pore structure of the sediment, as suggested by Kettridge et al. (2008). The colluvium overlying the interglacial Burtle Bed at Shapwick had a velocity of 0.057 m/ns, slower than that of the Burtle deposit of wet sand and clay at 0.073 m/ns. A velocity of 0.05 m/ns and dielectric permittivity of 35.95 was calculated for the silty clay wetland sediment at Caldicot and Marsal. This has a low level of confidence as the signal was becoming attenuated at the depth the corer was inserted to. These values for clay are at the upper end of the range given by Conyers (2004) and Mussett and Khan (2000) of 5–40 despite the sediment not being fully waterlogged.

The Topp equation is considered inappropriate for clays and organic rich soils below the water table with preference given to the CRIM model (Friedman, 1998; Troinke and Hamann, 2014). This research demonstrates the lack of correlation between the theoretical moisture content calculated from dielectric conductivity by both these models and the water content measured from gravimetric means on the bulk samples taken (Table 8). For both Annaghbeg and Castlegar (ombrotrophic peat) the Topp equation actually gives a better approximation of water content than the CRIM formula; however both overestimate the true moisture content. The CRIM formula gives very accurate moisture content at Shapwick (fen peat), while the Topp equation overestimates the moisture content for this site. The reverse is true for Caldicot where the Topp equation gives the correct value, while both overestimate the moisture content for Marsal, possibly due to the effect of high conductivity at this site. This demonstrates that although GPR has the potential to be used for monitoring wetland sites preserved in-situ (see results of survey at Shapwick Heath) it is important that GPR data are calibrated appropriately.

From the velocity and dielectric permittivity values the coefficients of reflectivity (R) between different types of sediment are calculated (Table 9). This shows that the greatest level of reflectance (R value = 0.27) should come from saturated fen peat overlying silty sand. This is the nature of the deepest anomaly identified in the GPR data at Shapwick where fen peat overlies a sandy Burtle which was identified as a strong reflector. This is greater than the values given in Table 4 which predict an R value of − 0.23 for marsh over wet sand, due to the much lower dielectric permittivity given for marsh than found for peat in this study. Colluvium in ombrotrophic peat or dry fen peat should also produce a strong reflector, and this was observed at Shapwick. While colluvium in saturated fen peat is not as strong, it is still sufficiently high as to produce a reflection as is dry fen peat in clay. The fen to ombrotrophic peat transition also has a high reflection coefficient and this was identified (although inconstantly) in the data collected at both Annaghbeg and Castlegar. It should be noted that these values are calculated assuming an abrupt boundary between the two sediment types. Wood has a small positive reflection coefficient in ombrotrophic peat but a high negative R value in dry fen peat and a lower value in clay. Wood roots were detected in clay at Caldicot, demonstrating that while these R values give a good indication of the strength of signal expected they should not be completely relied upon, particularly where the degree of preservation is unknown, as this can drastically alter the water content, and therefore dielectric permittivity, of wood.

The key geochemical indicators of anthropogenic activity include phosphorus, calcium, aluminium, sodium and some other metals. Peaks in phosphorus concentration were clearest at Castlegar where a peak in phosphorous concentration at 0.96–1.12 m was found in association with roundwoods. Excluding the high concentrations at the surface, this was the highest concentration in the sequence at 424.36 μg/L, and was the only point in the sequence where the correlation between phosphorus and potassium concentrations was interrupted (phosphorus usually mirrors potassium although potassium should be higher in ground water i.e. near the base of the sequence). At Caldicot a peak in

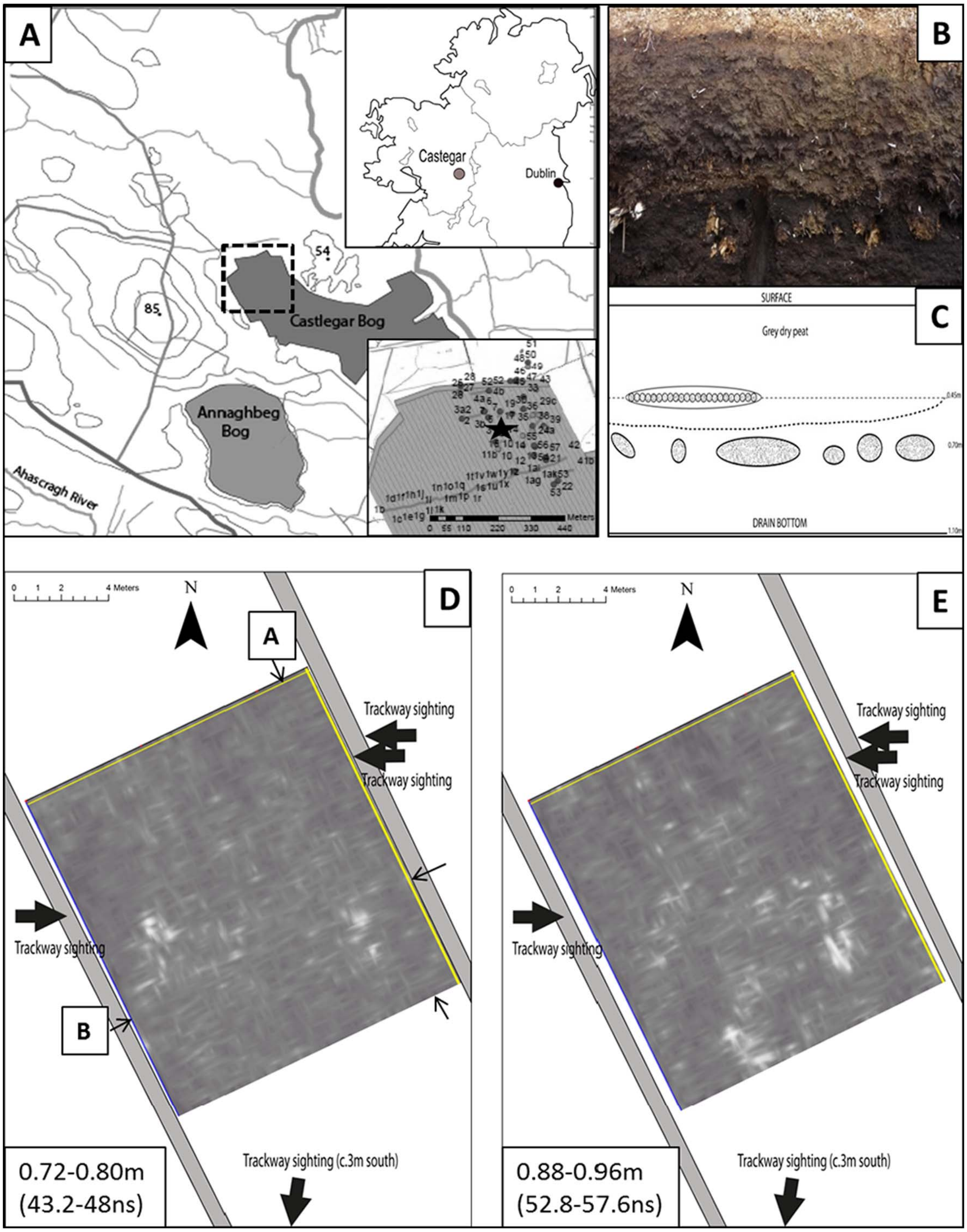

Fig. 5. A; The location of Annaghbeg and Castlegar bogs, Ireland, with locations of archaeological sightings in the west arm of Castlegar bog from Rohan (2009) inset on the right corner. The location of the survey grid is indicated by a black star. B and C; Photo and schematic of the East trackway sighting suggesting two separate structures. D and E; time slices (15 m × 12 m) of the data collected the borehole was taken at the point where the two intersect. Black indicates high amplitude and white indicates low amplitude.

phosphorus was observed and correlates to the depth of a GPR anomaly interpreted as a continuation of one of the structures revealed in the lake excavations. Higher organic matter content was also found at this depth in the sequence.

Peaks in calcium concentration are seen for one of the trackways at Castlegar and a wood peat layer at Shapwick. These indicate the introduction of material from the surrounding dry land areas through human or animal activity, suggesting a more stable surface. Peaks of aluminium and sodium concentrations were found associated with trackways at Castlegar and Caldicot, and Castlegar and Shapwick respectively. Both may indicate periods of slow sediment accumulation where the surface would have been more stable and able to support higher order plants as they are introduced from the atmosphere if under an oceanic climate, for example a surface peak was observed at Caldicot. More focused studies would need to be conducted to confirm this. The presence of a mobile water table in wetland contexts is liable to complex the geochemical signature. For example the high concentrations of potassium, aluminium, iron and copper associated with

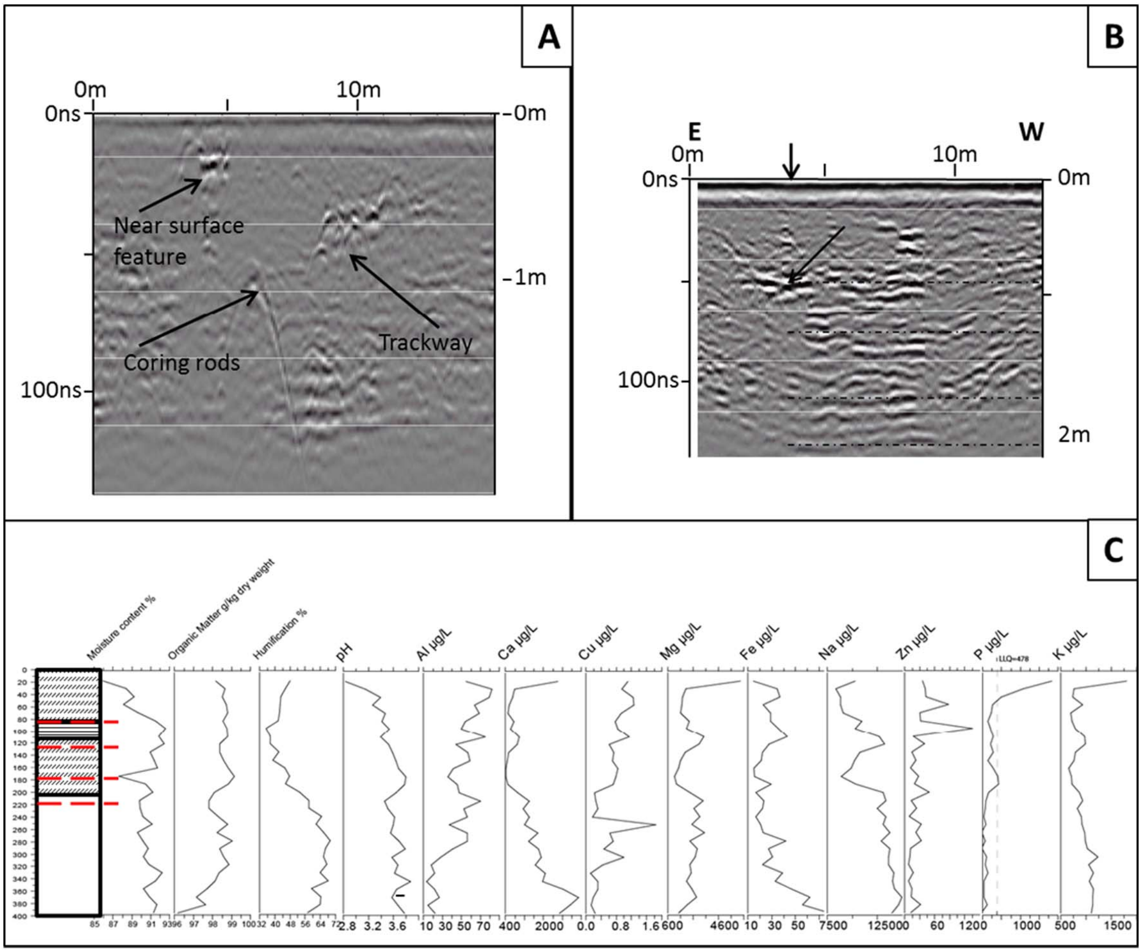

Fig. 6. A; Profile collected for calculation of velocity, the coring rods were inserted at a depth of 1 m (location is indicated by small arrows in Fig. 5D). B; 200 MHz GPR profile intersecting the trackway, dashed lines indicate potential stratigraphic boundaries (location is indicated by small arrows in Fig. 5D). C; The geochemical and physical profile of the core, red dashed lines show location of stratigraphic boundaries in GPR profile. (For interpretation of the references to colour in this figure legend, the reader is referred to the web version of this article.)

the anomaly at 0.24 m depth at Caldicot and a peak in a range of elements (Al, Ca, Cu, Fe, Mg and Na) observed in association with the anomaly at 0.56–0.72 m at Castlegar, interpreted as archaeological structures may equally be due to the presence of the water table at these sites. Being able to detect the watertable and its proximity to archaeological structures is important when considering the risk of degradation to that structure.

To be sure the above indicators are representative of anthropogenic activity it is essential to establish background variations. The range of the concentrations found in the cores at each site is presented in Table 10. Large variations in background geochemistry, both with depth and laterally, associated with different depositional sedimentary units, are demonstrated over a single site. This needs to be considered when designing the survey methodology by modelling from desk based assessments. Temporal variations have been found to be minimal where they were monitored at Annaghbeg (Milton, 2015) and Shapwick Heath (Jones, 2013). This implies that while changes in the background levels of geochemistry are expected between and across sites they do not seem to vary over time. It was not possible to carry out temporal monitoring at Castlegar, Caldicot or Marsal.

The results presented here generally support the pattern given above. Ombrotrophic bog samples have generally lower concentrations of all elements than the other sites (Table 10). High surface concentrations of calcium were observed at all sites and are higher in fen peat than ombrotrophic peat while magnesium concentrations decreased with depth in similar quantities allowing the Ca:Mg ratio to be used to identify the fen to bog transition. At Castlegar the ratio is approximately 1:1 at c.2 m which is a feasible depth for the fen to bog transition based on analysis of the peat vegetation. Where the underlying geology of a bog is calcareous pH is also a useful indicator for the presence of the fen to bog transition, an increase of pH with depth was observed at all three of the peat sequences.

The fen peat at Shapwick generally had a higher concentration of iron than the ombrotrophic peat at Annaghbeg and Castlegar, however, the aluminium concentration was also higher (although some much lower values were also found). Both Marsal and Caldicot had generally higher concentrations of both aluminium and iron than the peat at the other three sites. The marine clays at Marsal had much higher concentrations of iron, sodium and sulphate and much higher conductivity than the peat deposits and the fresh water clay at Caldicot. Some of the core samples at Shapwick also show high concentrations of sodium, sulphate and calcium indicating the presence of marine deposits/intrusion. Calcium concentrations were highest at Shapwick in association with the sandy interglacial Burtle Beds. Ground water run-off may also include high concentrations of sulphate (without increased concentration of calcium) depending on the geology of the catchment and pollution (Brown et al., 2010).

6. Conclusion

There is no denying the fact that GPR results from wetland contexts are often very unclear, and as such extremely difficult to interpret when

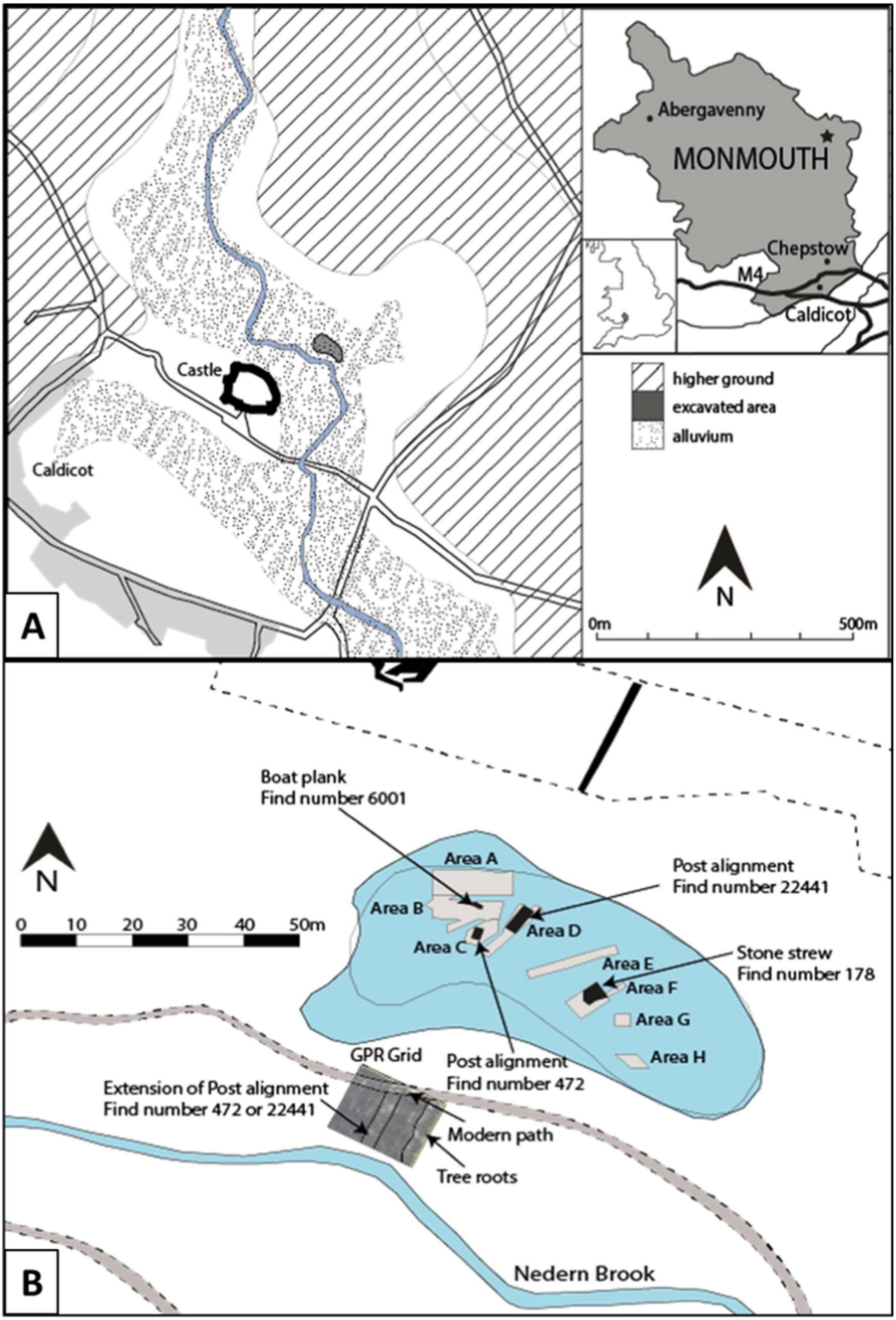

Fig. 7. A; The location of the lake and castle at Caldicot, Wales. B; The location of the GPR grid in relation to the structures revealed in the lake excavation (Nayling and Caseldine, 1997) and anomalies in GPR data collected to the north of the lake by Mansfield (2007).

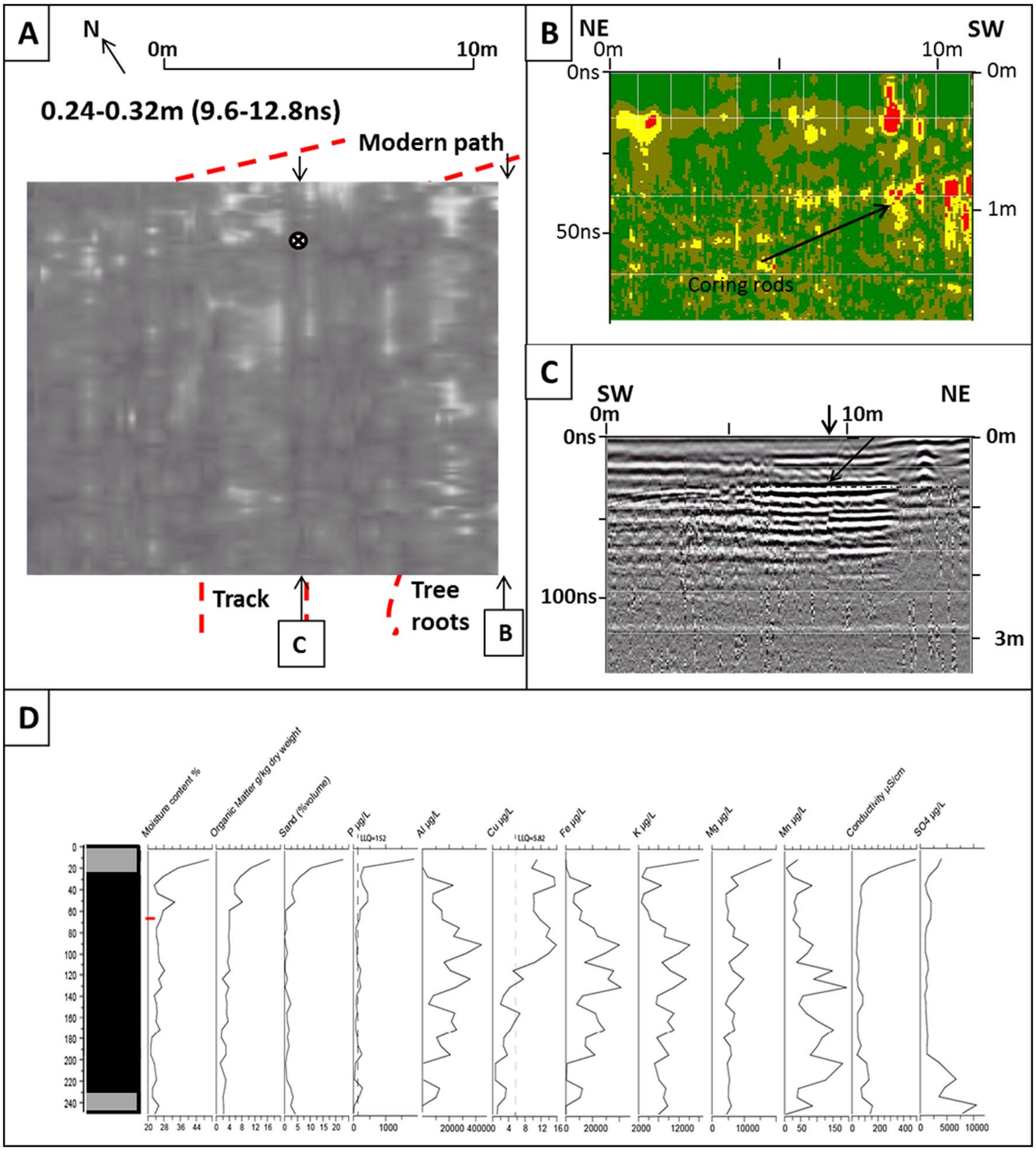

Fig. 8. A; A time slice of the GPR data grid showing anomalies interpreted as a modern path, trackway and tree roots. The core was collected at the point where the modern path and trackway intersect. B; The GPR profile used for calculating velocity, the cores were inserted at a depth of 1 m. C; A GPR profile intersecting the location of the borehole, large arrow indicates the borehole location. D; The geochemical and physical profile of the core, red dashed lines show location of stratigraphic boundaries in GPR profile Black indicates high amplitude and white indicates low amplitude in A and red shows high amplitude in B. (For interpretation of the references to colour in this figure legend, the reader is referred to the web version of this article.)

Table 7
Velocities (m/ns) and dielectric permittivities, calculated for the wetland sediments encountered in this research.

Sediment	Highly water logged		Wet		Dry	
	EM velocity	Dielectric permittivity	EM velocity	Dielectric Permittivity	EM velocity	Dielectric permittivity
Ombrotrophic peat	0.033	81.05	0.033	81.05		
Fen peat	0.042–0.045[a]	50.95	0.047-0.051[a]	40.69-34.56	0.067	20.23
Wood peat			0.040[a]	56.18		
Colluvium			0.057[a]	27.66		
Clay			0.05	35.95	0.05	35.95
Sandy clay			0.073[a]	16.87		

[a] Value from CMP data collected at Shapwick Heath.

Table 8
Comparison of moisture content values calculated from the gravimetric method compared to those calculated from dielectric permittivity using the Topp equation and CRIM formula for the surface metre at each site.

Site (K_a)	Average measured water content for the surface metre (%)	Averaged measured water content for surface metre (m^3/m^3)	Moisture content calculated by Topp (m^3/m^3)	Moisture content calculated by CRIM (m^3/m^3)[a]
Annaghbeg (81.05)	93.57	0.91	0.97	1.01
Castlegar (81.05)	90.11	0.76	0.97	1.01
Shapwick (50.95)	81.34	0.75	0.57	0.75
Caldicot (35.95)	28.62	0.48	0.48	0.56
Marsal (35.95)	27.28	0.36	0.48	0.56

[a] For Annaghbeg, Castlegar and Shapwick a K_m of 3 (that of dry silt) is used and for Caldicot and Marsal a K_m of 5 (that of dry clay) is used.

Table 9
The reflectivity of wetland sediments.

Overlying material	Underlying material	R value
Dry fen peat (20.23)	Colluvium (27.66)	0.27
Saturated fen peat (50.95)	Silty sand (16.87)	0.27
Ombrotrophic peat (81.05)	Colluvium (27.66)	0.26
Ombrotrophic peat (81.05)	Colluvium (27.66)	0.26
Saturated fen peat (50.95)	Colluvium (27.66)	0.15
Clay (30.95)	Dry fen peat (20.23)	0.14
Clay (30.95)	Dry fen peat (20.23)	0.14
Ombrotrophic peat (81.05)	Saturated fen peat (50.95)	0.12
Ombrotrophic peat (81.05)	Wood (56.18)	0.09
Saturated fen peat (50.95)	Clay (35.95)	0.09
Dry fen peat (20.23)	Silty sand (16.87)	0.05
Saturated fen peat (50.95)	Wood (56.18)	− 0.02
Dry fen peat (20.23)	Clay (35.95)	− 0.08
Clay (30.95)	Saturated fen peat (50.95)	− 0.09
Clay (30.95)	Wood (56.18)	− 0.11
Dry fen peat (20.23)	Wood (56.18)	− 0.25

compared to results from dryland sites. The GPR is operating at the limit of its capabilities, the results are therefore ambiguous and making interpretations based on radargrams alone is particularly challenging. Characterisation of the deposits prior to full survey is therefore an essential step in conducting geophysical surveys in wetlands. The results presented in this paper show a range of dielectric permittivities associated with different wetland sediment types from which a more accurate prediction of the potential to detect wooden structures and colluvium layers can be made. For example the detection of wood in saturated fen peat is less likely to be successful than detecting wood in clay, ombrotrophic peat or dry fen peat. Colluvium is likely to be detected if the overlying sediment is peat. As the results have shown, the analysis of borehole material, including geochemical analysis, can bridge the gap between geophysics results and archaeological interpretations to allow the successful application in wetland conditions. This can be used by curatororial, commercial and academic stakeholders for wetland heritage management and research. The results presented here, despite being more accurate than those currently found in the literature, are still in need of refinement and it is hoped that future work will address this. For example, this research has only dealt with a small range of sediment types and site conditions. Further GPR in wetland contexts should include full descriptions of sediments and independent analysis of velocity fields and moisture content to allow more detailed modelling of GPR responses in different conditions. The geochemistry results generally support the characteristics identified in the literature review but are still very vague. Focused geochemical studies on wetland sites subject to full excavation and interpretation could drastically improve the potential of employing these techniques as a means of interpreting different deposit types.

Archaeological structures in wetlands tend to be fragmentary in nature so using GPR in an exploratory capacity is unlikely to be a cost effective approach due to the high cross line sample density needed to provide convincing results. Indeed the results presented here would benefit from a smaller transect spacing to meet the Nyquist limit. Other geophysics techniques such as electromagnetic imaging (EM) allow a much more rapid coverage of large areas from which areas of archaeological potential within the wetland (i.e. the wetland to dryland interface and possible bridging points) can be identified for more detailed survey with GPR or excavation. This research has shown the potential of GPR to identify relationships between structures, as at Castlegar, or the presence of an extension of a known structure, as at Shapwick Heath, where excavation is either too costly or presents to great a risk to preservation. In this capacity of detailed area survey it is essential that the spacing between each survey transect does not exceed the Nyquist limit to improve signal to noise ratio.

Acknowledgements

This work was supported in part by the NERC GEF facility (loan 991) and funded by a University Home Studentship in Science at the University of Reading.

The author would like to thank Dr. Nick Branch and Dr. Steve Robinson for their guidance and support during this research. The author would also like to thank Dr. Tim Astin and Prof Penny Johnes for their inputs at the initial stages and Prof. Martin Bates for advice at the latter stages. Much gratitude is given to David Thornley for training in the use of GPR and Dr. Neil Linford (Historic England) for his advice on

Table 10
The range of soil solution concentrations in the core samples at each site.

Site	Marsal	Caldicot	Shapwick	Castlegar	Annaghbeg
Al (μg/L)	63.22–698,653.79	10.17–44,175.40	< 0.01–83,003.97	13.57–82.2	35.20–180.91
Ca (μg/L)	6395.52–42,237.79	3806.69–61,068.00	11,711.89–178,184.01	420.53–3482.80	464.86–7640.68
Cu (μg/L)	2.27–354.92	0.68–15.85	0.15–61.15	0.13–1.85	< 0.01–3.01
Fe (μg/L)	72.55–565,720.18	113.11–41,393.90	155.45–38,918.22	14.64–77.71	10.38–147.59
K (μg/L)	6418.02–336,759.73	2705.46–17,042.13	1895.84–54,251.84	661.94–1801.03	270.37–58,728.52
Mg (μg/L)	4541.87–286,784.90	3777.05–18,616.93	4103.38–28,571.27	1127.71–6329.69	2007.26–10,540.84
Mn (μg/L)	2.35–2462.70	4.00–193.31	9.12–747.70	< 0.01–5.33	0.38–293.05
Na (μg/L)	6404.11–1,362,129.08	1820.53–4441.96	5157.50–31,433.64	8370.98–14,950.56	0.49–22,145.41
P (μg/L)	64.87–12,722.53	4.34–1898.89	< 0.01–1781.98	< 0.01–1845.67	224.76–9983.73
SO_4 (μg/L)	2347.30–306,685.65	901.59–10,514.45	5162.27–135,314.69	3363.95–8590.72	0.15–13,428.47
Zn (μg/L)	20.65–1178.69	15.94–139.07	10.89–125.09	7.65–135.38	8.54–4635.11

this work and assistance with data processing. The following kindly granted permission for field work to be carried out: English Heritage, Natural England, Bord na Mona, National Archaeological Museum Saint-Germain-en-Laye and Monmouthshire County Council. The author would also like to thank the following for field assistance: Phil Stastney, Daniel Young, Enda Lydon, Ben Milton, Kevin Williams, Naomi Riddiford, Dave Thornley, Nick Branch and Mike Simmonds.

References

Amendas, G., McConnachie, G., Pournou, A., 2013. Selective reburial: a potential approach for the in situ preservation of waterlogged archaeological wood in wetland excavations. J. Archaeol. Sci. 40, 99–108.
Armstrong, K., 2010. Archaeological Geophysical Prospection in Peatland Environments. (Unpublished PhD thesis, Bournemouth University).
Bates, M.R., Bates, C.R., Whittaker, J., 2007. Mixed method approaches to the investigation and mapping of buried quaternary deposits: examples from Southern England. Archaeol. Prospect. 14, 104–129.
Bengtsson, L., Enell, M., 1986. Chemical analysis. In: Berglund, B.E. (Ed.), Handbook of Holocene Palaeoecology and Palaeohydrology. Wiley and Sons.
Bethell, P.H., Smith, J.U., 1989. Trace-element analysis of an inhumation from Sutton Hoo, using inductively coupled plasma emission spectrometry: an evaluation of the technique applied to analysis of organic residues. J. Archaeol. Sci. 16 (1), 47–56.
Bradley, R., 1990. The Passage of Arms. An Archaeological Analysis of Prehistoric Hoards and Votive Deposits. Cambridge.
Brown, A.G., Ellis, C., Roseff, R., 2010. Holocene sulphur-rich palaeochannel sediments: diagenetic conditions, magnetic properties and archaeological implications. J. Archaeol. Sci. 37, 21–29.
Bunting, C.J., 2012. Shapwick Burtle, Somerset: Report on Geophysical Survey, May 2012. (Unpublished report held at Somerset HER).
Chambers, F.M., Beilman, D.W., Yu, Z., 2011. Methods for determining peat humification and for quantifying peat bulk density, organic matter and carbon content for palaeostudies of climate and peatland carbon dynamics. Mires Peat 7 (7), 109–119.
Chapman, H., Adcock, J., Gater, J., 2009. An approach to mapping buried prehistoric palaeosols of the Atlantic seaboard in Northwest Europe using GPR, Geoarchaeology and GIS and the implications for heritage management. J. Archaeol. Sci. 36, 2308–2313.
Clymo, R.S., 1983. Peat. In: Gore (Ed.), Mires: Swamp, Bog, Fen and Moor. General Studies, Ecosystems of the World 4A. Elsevier, Oxford, pp. 159–224.
Coles, J.M., Hibbert, F.A., Orme, B.J., 1973. Prehistoric Roads and Tracks in Somerset, England: 3. The Sweet Track, Proceedings of the Prehistoric Society. Vol. 39. pp. 256–293.
Conway, J.S., 1983. An investigation of soil phosphorus distribution within occupation deposits from a Romano-British hut group. J. Archaeol. Sci. 10 (2), 117–128.
Conyers, L.B., 2004. Ground-Penetrating Radar for Archaeology. Altamira Press, Plymouth.
Crowther, J., 1997. Soil phosphate surveys: critical approaches to sampling, analysis and interpretation. Archaeol. Prospect. 4, 93–102.
Davis, J.L., Annan, A.P., 1989. Ground-penetrating radar for high-resolution mapping of soil and rock stratigraphy. Geophys. Prospect. 37, 531–551.
Dewis, J., Freitas, F., 1970. Physical and chemical methods of soil and water analysis, food and agriculture organization of the United Nations. Soils Bull. 10, 37.
Eberi, M., Alvarez, M., Terry, R.E., 2012. Chemical signatures of Middens at a Late Classic Maya Residential Complex, Guatemala. Geoarchaeology 27, 426–440.
English Heritage, 2008. Geophysical Survey in Archaeological Field Evaluation, 2nd ed. .
Entwistle, J.A., 2000. The Geoarchaeological significance and spatial variability of a range of physical and chemical soil properties from a former Habitation Site, Isle of Skye. J. Archaeol. Sci. 27, 287–303.
Entwistle, J.A., Abrahams, P.W., Dodgshon, A., 1998. Multi-element analysis of soils from Scottish historical sites. Interpreting land-use history through the physical and geochemical analysis of soil. J. Archaeol. Sci. 25, 53–68.
Farswan, Y.S., Nautiyal, V., 1997. Investigation of phosphorous enrichment in the burial soil of Kumaun, Mid-Central Himalaya, India. J. Archaeol. Sci. 24, 251–258.
Friedman, 1998. A saturation degree- dependent composite spheres model for describing the effective dielectric constant of unsaturated porous media. Water Resour. Res. 34 (11), 2949–2961.
Fyfe, R., Woodbridge, J., Rowe, J., 2010. Archaeological and Palaeoecological Survey at Hangingstone Hill, Winney's Down and Broad Down, Dartmoor. Unpublished report, School of Geography, Earth and Environmental Sciences, University of Plymouth.
GSSI, 2002. SIRVeyor SIR-20 User's Manual. North Salem, NH.
Haslam, R., Tibbett, M., 2004. Sampling and analyzing metals in soils for archaeological prospection: a critique. Geoarchaeology 19 (8), 731–751.
Henman, J., Poulter, B., 2008. Inundation of freshwater peatlands by sea level rise: uncertainty and potential carbon cycle feedbacks. J. Geophys. Res. 113, G01011.
Hodgson, J.A., Donohue, S.O., Connell, Y., Krahn, H., Reid, G., Young, M., 2009. A geophysical journey around Ireland. First Break 27, 35–42.
Holliday, V.T., Gartner, W.G., 2007. Methods of soil P analysis in archaeology. J. Archaeol. Sci. 34, 301–333.
Jones, L., 2013. An Evaluation of In Situ Preservation Potential and Monitoring Strategies at the Sites of the Sweet Track, and Glastonbury Lake Village, in the Somerset Levels, UK. (Unpublished PhD thesis, University of Reading).
Kettridge, N., Comas, X., Baird, A., Slater, L., Strack, M., Thopson, D., Jol, H., Binley, A., 2008. Ecohydrologically important subsurface structures in peatlands revealed by ground-penetrating radar and complex conductivity surveys. J. Geophys. Res. 113, G04030.
Konrad, V.A., Bomichsen, R., Clay, V., 1983. Soil chemical identification of ten thousand years of prehistoric human activity areas at the Munsungun Lake Throughfare, Maine. J. Archaeol. Sci. 10 (1), 13–28.
Kowalczyke, S., Lukasiak, D., Zukowska, K., 2014. In: Ground penetrating radar survey in the central and eastern part of the Calowanie Fen, Central Poland. Proceedings of the 15th International Conference on Ground Penetrating Radar-GPR 2014, Université catholique de Louvain. pp. 1041–1047.
Leckebusch, J., 2003. Ground-penetrating radar: a modern three-dimensional prospection method. Archaeol. Prospect. 10, 213–240.
Leonardi, G., Miglavacca, M., Nardi, S., 1999. Soil phosphorus analysis as an integrative tool for recognizing buried ancient Ploughsoils. J. Archaeol. Sci. 26, 343–352.
Lillie, M., Ellis, S., 2007. Wetland Archaeology and Environments: Regional Issues, Global Perspectives. Oxbow Books.
Mansfield, C., 2007. Reconstructing Buried Alluvial Landscapes: The Application of Multiple Geophysical and Geoarchaeological Techniques. (Unpublished PhD Thesis, Department of Archaeology, SHES, University of Reading).
Mansfield, C., 2009. Geophysical prospection of the bronze age site at Caldicot, Monmouthshire. In: Archaeology in the Severn Estuary. Vol. 20. pp. 81–97.
Matthiesen, H., 2008. Detailed chemical analysis of groundwater as a tool for monitoring urban archaeological deposits: results from Bryggen in Bregen. J. Archaeol. Sci. 35, 1378–1388.
Menotti, F., 2012. Wetland Archaeology and Beyond: Theory and Practice. Oxford University Press.
Mighall, T.M., Dumayne-Peaty, L., Cranstone, D., 2004. A record of atmospheric pollution and vegetation change as recorded in three peat bogs from the Northern Pennines Pb-Zn Orefield. Environ. Archaeol. 9, 13–38.
Milner, N., Conneller, C., Elliott, B., Koon, H., Panter, I., Penkman, K., Taylor, B., Taylor, M., 2011. From riches to rags: organic deterioration at Star Carr. J. Archaeol. Sci. 38, 2818–2832.
Milton, C.J., 2015. Quantifying the Heritage Resource Potential of Lowland Wetlands in North West Europe: An Integrated Geophysical, Geoarchaeological and Geochemical Approach. (Unpublished PhD thesis, University of Reading).
Mussett, Khan, 2000. Looking Into the Earth: An Introduction to Geological Geophysics. Press, Cambridge University.
Nayling, N., Caseldine, A., 1997. Excavations at Caldicot, Gwent: Bronze Age Palaeochannels in the Lower Nedern Valley, CBA Research Report 108. Council for British Archaeology, York.
Olivier, L., Kovacik, J., 2006. The 'Briquetage de la Seille' (Lorraine, France): proto-industrial salt production in the European iron age. Antiquity 80, 558–566.
Oonk, S., Slomp, C.P., Huisman, D.J., 2009. Geochemistry as an aid in archaeological prospection and site interpretation: current issues and research directions. Archaeol. Prospect. 16, 35–51.
O'Sullivan, A., 1998. The Archaeology of Lake Settlement in Ireland (Discovery Programme Monographs 4). Royal Irish Academy, Dublin.
Parnell, J.J., Terry, R.E., Golden, C., 2001. Using in-field phosphate testing to rapidly identify Middens at Piedras Negras, Guatemala. Geoarchaeology 16 (8), 855–876.
Patrick, W.H., Mahapata, I.C., 1968. Transformations and availability to rice of nitrogen and phosphorous of waterlogged soils. Adv. Agron. 20, 323–359.
Persson, K.B., 1997. Soil phosphate analysis: a new technique for measurement in the field using a test strip. Archaeometry 39 (2), 441–443.
Plado, J., Sibul, I., Mustasaar, M., Joeleht, A., 2011. Ground-penetrating radar study of the Rahivere peat bog, eastern Estonia. Estonian J. Earth Sci. 60 (1), 31–42.
Reflexw, 2012. (Version 7.1.4c) (software). Karlsruhe, Germany: Sandmeier Scientific Software. Retrieved from. http://www.sandmeier-geo.de/download.html.
Riddiford, N.G., Branch, N.P., Williams, K., Bunting, C.J., Smith, M., 2012. Project Briquetage de la Seille 2012: Geoarchaeological and Biostratigraphic Investigations. (Unpublished report, University of Reading).
Rohan, N., 2009. Peatland Survey 2007 and 2008 Blackwater, Derryfadda, Coolnagun, Moutdillon Group of Bogs, Counties Offaly, Galway, Longford, Westmeath and Roscommon. pp. 19–50 (ADS).
Sharpley, A.N., Kleinman, P.J.A., Weld, J.L., 2008. Environmental soil phosphorus indicies. In: Carter, M.R., Gregorich, E.G. (Eds.), Soil Sampling and Methods of Analysis, second edition. Canadian Society of Soil Science, pp. 141–145.
Styles, P., 2012. Environmental Geophysics: Everything you Ever Wanted (Needed!) to Know but Were Afraid to Ask!. EAGE, Netherlands.
Sullivan, K.A., Kealhofer, L., 2004. Identifying activity areas in archaeological soils from a colonial Virginia house lot using phytolith analysis and soil chemistry. J. Archaeol. Sci. 31, 1659–1673.
Terry, R.E., Fernández, F.G., Parnell, J.J., Inomata, T., 2004. The story in the floors: chemical signatures of ancient and modern Maya activities at Aguateca, Guatemala. J. Archaeol. Sci. 31, 1237–1250.
Theimer, B.D., Nobes, D.C., Warner, B.G., 1994. A study of the geoelectrical properties of peatlands and their influence on ground-penetrating radar surveying. Geophys. Prospect. 42, 179–209.
Topp, G.C., Davis, J.L., Annan, A.P., 1980. Electromagnetic determination of soil water content: measurements in coaxial transmission lines. Water Resour. Res. 16 (3), 574–582.
Tröels-Smith, J., 1955. Karakterisering af løse jordarter Danmarks. Geologiske Undersøgelse Series IV 3 (10) (73 pp).
Troinke, J., Hamann, G., 2014. In: Deriving hydrological parameters from VRP data: accounting for uncertainties in inverted velocities and petrophysical models. Proceedings of the 15th International Conference on Ground Penetrating Radar-GPR 2014, Université catholique de Louvain. pp. 176–180.
Utsi, E., 2004. Ground-penetrating radar time-slices from North Ballachulish Moss.

Archaeol. Prospect. 11, 65–75.
Van de Noort, R., O'Sullivan, A., 2006. Rethinking Wetland Archaeology. Gerald Duckworth and Co. Ltd., London.
Van de Noort, R., Chapman, H.P., Cheetham, J.L., 2001. In situ preservation as a dynamic process: the example of Sutton Common, UK. Antiquity 94–100.
Wells, J., Weir, D., Brunning, R., 1999. Unpublished, Excavation of a Possible Terminal of the Sweet Track and Pollen Analysis of Associated Mid-Holocene Peat (SW93). Somerset, Somerset HER.
Wilson, C.A., Davidson, D.A., Cresser, M.S., 2008. Multi-element soil analysis: an assessment of its potential as an aid to archaeological interpretation. J. Archaeol. Sci. 35, 412–424.
Young, D.S., Branch, N.P., Stastney, P., Black, S., Elias, S.A., 2011a. Archaeological Excavations at Longford Pass Bog, Co. Tipperary, Ireland: Environmental Archaeological Analysis, Quaternary Scientific (QUEST) Unpublished Report October 2011; Project Number 004/10.
Young, D.S., Branch, N.P., Stastney, P., Black, S., Elias, S.A., 2011b. Archaeological Excavations at Cloonshannagh Bog, Co. Roscommon, Ireland: Environmental Archaeological Analysis, Quaternary Scientific (QUEST) Unpublished Report October 2011; Project Number 004/10.
Young, D.S., Branch, N.P., Stastney, P., Black, S., Elias, S.A., 2011c. Archaeological Excavations at Killeen Bog, Co. Tipperary, Ireland: Environmental Archaeological Analysis, Quaternary Scientific (QUEST) Unpublished Report November 2011; Project Number 004/10.
Young, D.S., Branch, N.P., Stastney, P., Black, S., Elias, S.A., 2012a. Archaeological Excavations at Castlegar Bog, Co. Galway, Ireland: Environmental Archaeological Analysis, Quaternary Scientific (QUEST) Unpublished Report June 2012; Project Number 004/10.
Young, D.S., Branch, N.P., Stastney, P., Black, S., Elias, S.A., 2012b. Archaeological Excavations at Gowla Bog, Co. Galway, Ireland: Environmental Archaeological Analysis, Quaternary Scientific (QUEST) Unpublished Report July 2012; Project Number 004/10.
Young, D.S., Branch, N.P., Stastney, P., Black, S., Elias, S.A., 2012c. Archaeological Excavations at Killaderry Bog, Co. Galway, Ireland: Environmental Archaeological Analysis, Quaternary Scientific (QUEST) Unpublished Report July 2012; Project Number 004/10.